CLM-P698

CLM-P698

UKAEA

Preprint

ERGODIC BEHAVIOUR IN A MAGNETIC LIMITER

T. J. MARTIN
J. B. TAYLOR

CULHAM LABORATORY
Abingdon Oxfordshire
1983

CLM-P 698

ERGODIC BEHAVIOUR IN A MAGNETIC LIMITER

T J Martin and J B Taylor

Culham Laboratory, Abingdon, Oxon OX14 3DB, UK

(Euratom/UKAEA Fusion Association)

Abstract

The effect of "diffuser" coils which perturb the magnetic surfaces in a Tokamak - as in an "ergodic limiter" - is investigated by means of a simple model. This model leads to an area-preserving two parameter map with interesting invariance properties which describes the production of magnetic islands and of an ergodic layer. As the strength of the diffuser is increased the magnetic islands remain fixed but change their size in such a way that the overall pattern, and the boundary of the ergodic zone, move away from the diffuser. Analytic expressions are derived for this movement and for the location of the ergodic boundary.

(Submitted for publication in Plasma Physics)

July 1983

1. INTRODUCTION

One method for providing additional control over diffusion in the outer layers of the plasma in a large Tokamak such as JET is by localised coils which perturb the magnetic flux surfaces in the vicinity of the wall (FENEBERG, 1977; ENGELHARDT & FENEBERG, 1978; FENEBERG & WOLF, 1981). One class of such devices (BELITZ et al, 1982) consists of a grid of current carrying wires aligned with the unperturbed magnetic field lines in their vicinity, see Fig 1. The field of this grid can resonate with the main field so as to produce (i) rippling of the flux surfaces, (ii) island structures among the flux surfaces and (iii) ergodic* regions in which the flux surfaces are destroyed.

The effect of such a "diffuser" coil can be investigated by tracing field-lines but such calculations are restricted to specific situations. In order to illustrate the more general aspects of this type of diffuser we have constructed the model described in the next section. This contains the essential features of both the diffuser and the Tokamak and describes the influence of parameters such as rotational transform, shear, diffuser strength, diffuser periodicity and diffuser length. It also leads to an area preserving mapping problem with interesting invariance properties. Some details of this mapping are calculated in the Appendices.

2. THE MODEL

In the model we separate the influence of the diffuser and of the shear in the Tokamak field. The diffuser acts only over a small part of the toroidal circumference in which shear can be neglected. The shear acts over the remainder of the toroidal circumference where the diffuser field can be neglected. Thus the model has two regions.

---

*"Ergodic" is used in the colloquial sense current in plasma confinement studies, not implying any strict mathematical definition. "Stochastic" and "chaotic" are also used to describe these regions.

(i) The diffuser.

In this region there is a uniform field in the z direction together with transverse fields in the x and y directions. These transverse components are periodic in x and independent of z and are assumed to extend over a length ℓ. Specifically the diffuser field is

$$B_x = \frac{-m\pi I}{a} e^{\frac{-my}{a}} \cos\left(\frac{mx}{a}\right)$$

$$B_y = \frac{m\pi I}{a} e^{\frac{-my}{a}} \sin\left(\frac{mx}{a}\right) \qquad (1)$$

$$B_z = B_o$$

representing a diffuser grid of 'wave length' $2\pi a/m$ with a current I in each wire sinusoidally distributed across the wire. The parameter a corresponds to the minor radius of the Tokamak, x/a corresponds to the poloidal angle θ and y is distance from the grid, ie $y = (a - r)$.

In this diffuser region the equation of a field line is

$$\frac{dx}{dz} = \frac{-m\pi I}{aB_o} e^{\frac{-my}{a}} \cos\left(\frac{mx}{a}\right)$$

$$\frac{dy}{dz} = \frac{m\pi I}{aB_o} e^{\frac{-my}{a}} \sin\left(\frac{mx}{a}\right) \qquad (2)$$

Integrating these equations over the diffuser length ℓ shows that a field line entering the diffuser at (x_1, y_1) emerges at (x_2, y_2), where

$$x_2 = x_1 - \frac{m\pi\ell I}{aB_o} e^{\frac{-my_1}{a}} \cos\left(\frac{mx_1}{a}\right)$$

$$y_2 = y_1 + \frac{a}{m} \log\left\{\cos\left[\frac{mx_1}{a} - \frac{m^2\ell\pi I}{a^2 B_o} e^{\frac{-my_1}{a}} \cos\left(\frac{mx_1}{a}\right)\right]\right\} - \frac{a}{m} \log\left\{\cos\left(\frac{mx_1}{a}\right)\right\} \qquad (3)$$

This defines a "diffuser mapping" T_{12} of the field lines which enter the diffuser onto those leaving it. Of course this mapping has unit Jacobian and so is area (= flux) preserving.

(ii) The Tokamak.

After leaving the diffuser, a field line continues round the remainder of the torus under the influence of rotational transform and shear only; its position (x_2, y_2) will thus be mapped into (x_3, y_3) by a simple twist mapping T_{23},

$$x_3 = x_2 + \alpha + \beta y_2$$

$$y_3 = y_2 \qquad (4)$$

where α is the displacement of a field line due to rotational transform, equivalent to $2\pi a/q$, and β is the displacement due to shear, representing $(2\pi a/q^2)(dq/dr)$ in the real Tokamak.

Combination of the mappings T_{12} and T_{23} gives the mapping of field lines once around the complete torus. It is convenient to remove the inessential parameters by writing $X \equiv \frac{mx}{a}$ and $Y \equiv \frac{m}{a}(y + \alpha/\beta)$. (This places the origin $Y = 0$ at a point where the rotational transform is an integral multiple of $2\pi/m$). Then the model is described by the basic map $T_{12} \times T_{23} \equiv T$:

$$X_2 = X_1 - pe^{-Y_1} \cos X_1$$

$$Y_2 = Y_1 + \log\{\cos(X_1 - pe^{-Y_1} \cos X_1)\} - \log\{\cos X_1\} \qquad (5)$$

$$X_3 = X_2 + sY_2$$

$$Y_3 = Y_2$$

where

$$p = \frac{\pi m^2 \ell I}{a^2 B_o} \quad , \qquad \text{(measures the strength of the diffuser relative to the toroidal field.)}$$

and

$$s = \frac{2\pi a}{q^2} \frac{dq}{dr} \quad , \qquad \text{(measures the strength of the shear in the original Tokamak.)}$$

Note that the effect of the diffuser depends only on the two dimensionless parameters p and s.

3. BEHAVIOUR OF THE MODEL

We shall see that the model described above exhibits all the expected characteristics, including ergodic behaviour. It is therefore worth noting that <u>neither</u> of the two individual mappings T_{12} or T_{23} can ever themselves be ergodic. Of course the Tokamak map T_{23} was designed to have invariant (= magnetic) surfaces $\psi = y$. But the diffuser map T_{12} also has <u>exact</u> invariant surfaces given by

$$\psi(x,y) = e^{\frac{-my}{a}} \cos\left(\frac{mx}{a}\right) \quad . \qquad (6)$$

Furthermore, if we had considered simply a superposition of diffuser and Tokamak fields round the complete torus, the resultant field would still have possessed exact invariant surfaces, given by

$$\psi(x,y) = e^{\frac{-my}{a}} \cos\left(\frac{mx}{a}\right) + \alpha y + \beta y^2/2 \quad , \qquad (7)$$

an example of which is shown in Fig 2. It corresponds not to an ergodic limiter but to a simple magnetic divertor. It is only because the diffuser field is confined to part of the toroidal circumference that the model exhibits ergodic behaviour.

Turning to the mapping T itself we note that since it is periodic in X we need study it only in the interval $(0,2\pi)$. A second important point is that if pe^{-Y_1} exceeds unity then Y_2 may become complex! This corresponds to field lines which pass between, and encircle, the grid wires. We have discarded any such lines from the figures shown below. [Note that this phenomenon cannot occur if $pe^{-Y} < 1.$]

Some illustrations of the field line behaviour in our model are given in Figs 3-6. These show the results of iterating the mapping T some hundreds of times. The samples shown are for $s = 2\pi$, (a typical value for a Tokamak) and illustrate the effect of increasing diffuser strength. As might have been expected, in the zone closest to the diffuser the field lines are almost entirely chaotic. Further from the diffuser there is a zone of mixed chaotic field lines and complex "magnetic island" structures, while further still from the diffuser the Tokamak flux surfaces are almost entirely intact and only slightly rippled. As the strength of the diffuser is increased these zones move further away from the diffuser with a corresponding increase in the width of the chaotic region.

The behaviour described above is typical and expected; a quantitative explanation for it will be given in the next section. However it is important to realise that strikingly different structures can also be created by the diffuser. For example Fig 7 shows a case with very weak shear in which one obtains a very large magnetic island with strong deformation of the magnetic surfaces but an almost imperceptible chaotic region. It seems, therefore that the diffuser is effective in creating an ergodic zone when the shear is appreciable, but if shear is too weak it may only distort the surfaces and act more as a simple magnetic limiter.

The behaviour as the shear is increased, at fixed diffuser strength, is shown in Figs 8-10. The magnetic islands get smaller but there are more of them and the chaotic regions expand and engulf some of the islands.

4. INTERPRETATION

We now turn to the interpretation of these results. The mapping T is invariant under a (renormalisation like) group of discrete transformations:

$$Y \to Y + 2\pi k/s$$
$$p \to p \exp(2\pi k/s) \qquad (8)$$

where k is any integer. This invariance enables us to "translate" the results for one particular diffuser strength into results applicable to a whole sequence of stronger or weaker diffusers. This is already suggested by Figs 3 and 5. The ratio of the diffuser strengths in these two cases happens to be close to $\exp 2\pi/s$ and it will be observed that the patterns are similar if one of them is displaced by $\Delta Y \sim 2\pi/s$. For example the island structures at $Y \sim 0.5$ in Fig 3 appear at $Y \sim 1.5$ in Fig 5. A case in which the comparison is exact is shown in Figs 11 and 12, where the respective values of p differ by a factor of 100 but the patterns are identical.

This invariance property allows us to derive an important result concerning the location of the boundary of the stochastic region. If for some value of diffuser strength p the boundary occurs at Y_e, then if (log p) is increased by $2\pi/s$ the stochastic boundary is displaced a distance $2\pi/s$. Hence the general behaviour of the stochastic boundary is given by

$$\frac{dY_e}{d(\log p)} \sim \frac{\Delta Y_e}{\Delta(\log p)} = 1 \qquad (9)$$

leading to an explicit form for its position, viz

$$Y_e = g(s) + \log p \quad . \qquad (10)$$

We will later determine the function $g(s)$, but first we examine more carefully the meaning of this displacement of the stochastic boundary.

So far it has been shown that the stochastic boundary is displaced towards larger Y as p is increased, approximately according to Eq (9), and that the whole flux surface pattern is exactly displaced towards larger Y, when p is increased by $\exp(2\pi/s)$. One might conclude that this is simply because the field structures created by the diffuser move outwards as the diffuser strength is increased. This is not correct. To see this consider the location of the "magnetic islands". These are situated at fixed points of the mapping T. A sequence of such points is given by

$$X = \pi + pe^{-Y}\cos X$$

$$Y = \frac{2m\pi}{s} + \frac{p}{s}e^{-Y}\cos X \qquad (m = \text{integer}) \qquad (11)$$

and for $pe^{-Y} < 1$ they are approximately

$$X_m = \pi - pe^{-2m\pi/s}$$

$$Y_m = \frac{2m\pi}{s} - \frac{p}{s}e^{-2m\pi/s} \quad . \qquad (12)$$

Thus these islands are almost equally spaced at intervals of $2\pi/s$ along a line close to $X = \pi$ (this can be confirmed by close examination of the figures) and their location changes only very slightly as p is increased. How can this be reconciled with the overall outward displacement of the flux pattern as p increases? The answer is that the islands indeed do not move significantly as p increases; instead the size of each island changes, and the stochastic region round it grows, so that when p has increased by $e^{2\pi/s}$ each island resembles the island which was immediately below it before p increased. This together with the exponentially small change in the island position exactly restores the whole flux surface pattern but displaced by $2\pi/s$, the spacing between the corresponding islands.

The width of the islands can be calculated by a form of perturbation theory introduced by DUNNETT, LAING & TAYLOR (1968) - [see Appendix A]. In this way one finds that the width of the island centred at $\sim 2m\pi/s$ is

$$\Delta Y_m \sim \left(\frac{2p}{s}\right)^{1/2} \exp(-m\pi/s) \quad , \tag{13}$$

confirming that when p is increased by a factor $e^{2\pi/s}$ the width of the m^{th} island becomes identical with the width which the $(m-1)^{th}$ island had before p was increased.

One could also use this estimate of island width, together with the oft-quoted island overlap criterion (CHIRIKOV, 1979; ROSENBLUTH et al, 1966) for the onset of stochastic behaviour, to determine the location of the stochastic boundary. The spacing of the islands is $2\pi/s$ so that overlap occurs at

$$Y_e = \log\left(\frac{sp}{\pi^2}\right) \quad . \tag{14}$$

In fact this 'overlap' criterion is not a reliable one, although it gives the correct trend, and a more accurate estimate of the position of the stochastic boundary (defined as the last complete flux surface as one approaches the diffuser) can be obtained.

As shown in Appendix B, in an appropriate asymptotic limit the mapping T reduces to the simpler map

$$\begin{aligned} X' &= X + sY + \lambda \sin X \\ sY' &= sY + \lambda \sin X \end{aligned} \tag{15}$$

where $\lambda \equiv spe^{-Y}$. Replacing $X \to \theta$, $sY \to -\phi$ and taking the inverse, this becomes

$$\begin{aligned} \theta' &= \theta + \phi \\ \phi' &= \phi + \lambda \sin \theta' \end{aligned} \tag{16}$$

which is exactly the Chirikov-Taylor standard map which has been exhaustively studied [see example LICHTENBERG & LIEBERMAN, (1983)] and whose stochastic boundary is known with great precision to be $\lambda = 0.971635!$ (GREENE, 1979). Consequently for the present model a more reliable estimate of the location of the stochastic boundary is

$$Y_e = \log(sp) + 0.03 \quad . \tag{17}$$

In terms of the Tokamak parameters this means that the thickness of the stochastic layer is

$$\Delta r = \frac{a}{m} \log\left\{\frac{2\pi^2 m^2 \ell I}{aB_o} \cdot a \frac{d}{dr}\left(\frac{1}{q}\right)\Big|_a\right\} \tag{18}$$

Note that increasing either diffuser current or Tokamak shear produces a thicker stochastic layer.

5. APPLICATION

We now consider the application of this model to a large Tokamak such as JET. As an illustration we take the parameters of this to be

Minor Radius	a	= 100 cm
Major Radius	R	= 300 cm
Toroidal Field	B_o	= 25 kgauss
Poloidal Field	B_p	= 10 kgauss
Toroidal Current	I_t	= 5 M Amp

For the diffuser we assume a grid of wires at a spacing of 16 cm (wavelength 32 cm), and a length of 80 cm, each wire carrying a current of 100 kA. In our model these parameters correspond to

$$m \simeq 20, \quad p \simeq 4, \quad s \simeq 2\pi.$$

The corresponding surfaces are shown in Fig 13. For the same parameters Eq (18) predicts the thickness of the stochastic layer to be $\Delta r/a = 0.16$,

which is in excellent agreement with the figure. A comparison of the location of the stochastic boundary deduced from computer plots with the location predicted by Eq (17), for some 25 different cases, is shown in Fig 14 confirming that the agreement extends over a wide range, indeed for all sp > 1.

6. CONCLUSIONS

We have described a model which illustrates the effects produced by a grid-like diffuser coil which perturbs the magnetic surfaces in a Tokamak. This model leads to a two-parameter mapping which allows one to investigate the influence of diffuser current, diffuser length and diffuser periodicity as well as that of the Tokamak shear. The effectiveness of the diffuser is measured by

$$p = \frac{\pi\, m^2 \ell I}{a^2 B_o}$$

and that of the tokamak shear by

$$s = 2\pi a \cdot \frac{d}{dr}\left(\frac{1}{q}\right) .$$

For small shear the effect of a weak diffuser is to ripple the magnetic surfaces, creating a large island structure with associated separatrices but very little stochasticity - rather like a magnetic limiter. For more typical values of shear and stronger diffusers the effect is to create a fully stochastic zone near the diffuser, surrounded by a zone where both island structures and stochastic regions are present. As the diffuser strength is increased the location of these island structures is almost unchanged but their size alters in such a way that the overall effect is as if the complete pattern moved outwards.

A remarkable feature of this model is that by exploiting the invariance properties of the mapping one can describe all these effects analytically and determine the width of the stochastic layer.

REFERENCES

BELITZ H., DIPPEL K. H., FUCHS G. & WOLF G. H. (1982) Euratom Tokamak Workshop, Schliersee, Nov 1982

CHIRIKOV B. V. (1979) Phys. Reports 52, 265

DUNNETT D. A., LAING E. & TAYLOR J. B. (1968) J. Math. Phys. 9 1819

ENGELHARDT W. & FENEBERG W. (1978) J. Nucl. Mat. 76/77, 518

FENEBERG W. (1977) Controlled Fusion & Plasma Physics (Proc. 8th Europ. Conf. 1977) Vol 1, p3

FENEBERG W. & WOLF G. H. (1981) Nuc. Fusion 21, 669

GREENE J. M. (1979) J. Math. Phys. 20, 1183

LICHTENBERG A. J. & LIEBERMAN M. A. (1983) Regular & Stochastic Motion Springer-Verlag N. Y. 1983

ROSENBLUTH M. N., SAGDEEV R. Z., TAYLOR J. B. & ZASLAVSKI G. M. (1966) Nuclear Fusion 6, 207

APPENDIX

In this section we show how the widths of the magnetic islands may be determined by an appropriate form of perturbation theory and, most importantly, how the boundary of the ergodic zone may be determined in an appropriate asymptotic theory.

A Size of Magnetic Islands

The width of the magnetic islands at $X \sim \pi$, $Y \sim 2\pi m/s$ can be determined by perturbation theory, treating the diffuser field pe^{-Y} as small. [This is formally equivalent to expansion in powers of p.]

If the mapping T is formally expanded to first order in p it reduces to

$$x' = x + sy + g(x,y)$$
$$y' = y + h(x,y) \qquad \text{A1}$$

where

$$g \equiv spe^{-y} \sin x - pe^{-y} \cos x$$
$$h \equiv pe^{-y} \sin x \qquad \text{A2}$$

[N.B. this mapping is area preserving only to order p^2.] Now any flux surface $\phi(x,y)$ satisfies

$$\phi(x,y) = \phi(x + sy + g,\ y + h) \qquad \text{A3}$$

so if the flux surface is also expanded in powers of p;

$$\phi(x,y) = \phi^0(x,y) + \phi^1(x,y) + \ldots \qquad \text{A4}$$

we have

$$\phi^0(x,y) = \phi^0(x + sy,\ y) \quad . \qquad \text{A5}$$

But ϕ must be periodic in x so this can only be satisfied everywhere if ϕ^0 is a function of y only - as one expects since this represents the situation without any diffuser.

Then in first order

$$\psi^1(x,y) = \psi^1(s + sy,\ y) + h(x,y) \cdot \frac{\partial \psi^0}{\partial y} \quad . \qquad \text{A6}$$

[Note that ψ^1 depends only on $h(x,y)$ and not on $g(x,y)$.] Since ψ^1 is also periodic in x we can write

$$\psi^1 = \sum a_m(y) \cos mx + b_m(y) \sin mx \quad , \qquad \text{A7}$$

then from Eq (A6) one finds

$$\psi^1 = \frac{pe^{-y}}{2} \cdot \frac{\partial \psi_0}{\partial y} \cdot \frac{\cos(x - sy/2)}{\sin(sy/2)} \quad . \qquad \text{A8}$$

If, as in conventional perturbation theory, the unperturbed flux surfaces are taken to be given by $\psi^0(y) = y$ then ψ^1 diverges at each of the islands! As pointed out by DUNNETT, LAING & TAYLOR (1968) this divergence is a reflection of the fact that under the perturbation the <u>topology</u> of the flux surfaces must change. This change can be accommodated by making a suitable choice of the function $\psi^0(y)$, which is in reality arbitrary. In the present problem a proper choice is

$$\psi^0 = \cos(sy/2) \quad . \qquad \text{A9}$$

Then

$$\psi = \cos(sy/2) + \frac{spe^{-y}}{4} \cos(x - sy/2) \qquad \text{A10}$$

and is (to this order) finite. Since ψ is constant on a flux surface this yields the width of the magnetic island centred at $x = \pi$, $y = 2\pi m/s$ as

$$\Delta y = \left(\frac{2p}{s}\right)^{1/2} e^{-\pi m/s} \quad . \qquad \text{A11}$$

B Ergodic Boundary

As mentioned in the text, the above estimate of island size may be used in conjunction with the "island-overlap" criterion to estimate the position of the boundary of the ergodic zone. However a better estimate can be found as follows.

The calculation in section A above, essentially an asymptotic expansion in powers of p with $p \to 0$, is not really consistent since $y_e \to -\infty$ in this limit. The correct expansion for treating the ergodic boundary is one with $p = 0(\varepsilon)$ and $s = 0(1/\varepsilon)$ so that y_e remains finite as $\varepsilon \to 0$. The deformation of the flux surfaces is also $0(\varepsilon)$ in such an expansion so we must write $y = \bar{y} + \delta y$ with $s\delta y = 0(1)$. Then with this ordering the proper asymptotic limit for the mapping T, as $\varepsilon \to 0$ is

$$x' = x + sy + spe^{-\bar{y}} \sin x$$

$$sy' = sy + spe^{-\bar{y}} \sin x \quad . \qquad \text{B1}$$

Or

$$x' = x + z'$$

$$z' = z + \lambda \sin x \qquad \text{B2}$$

where $\lambda \equiv sp \exp(-\bar{y})$. Note that this asymptotic map, unlike (A1), is <u>exactly</u> area-preserving. It is also a form of the well-known Chirikov-Taylor standard map whose properties have been extensively studied and for which the ergodic boundary is known to be $\lambda = \lambda_c = 0.971635$.

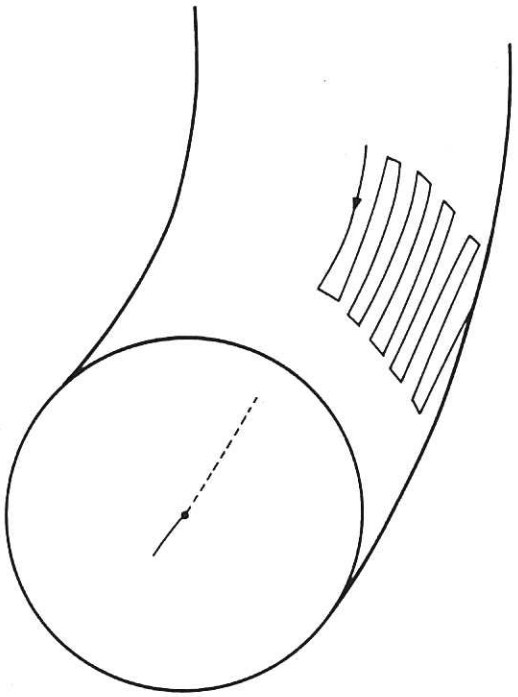

Fig.1a Arrangement of diffuser coils in a Tokamak.

Fig.1b The model coordinate system.

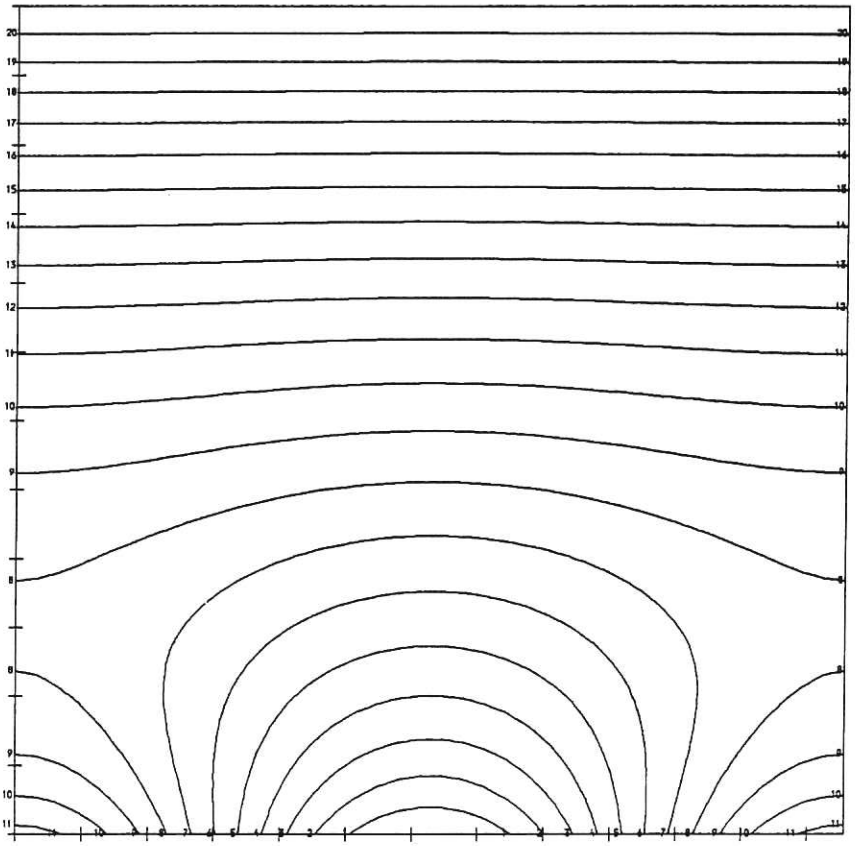

Fig.2 The effect of superposition of diffuser and Tokamak maps.

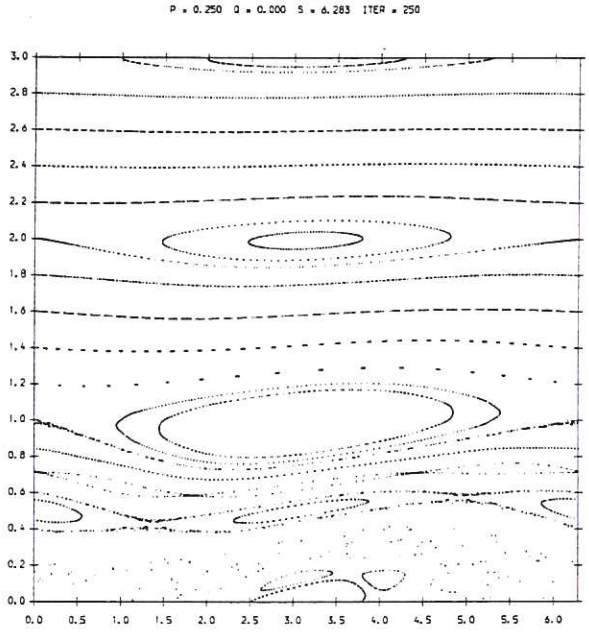

Fig.3

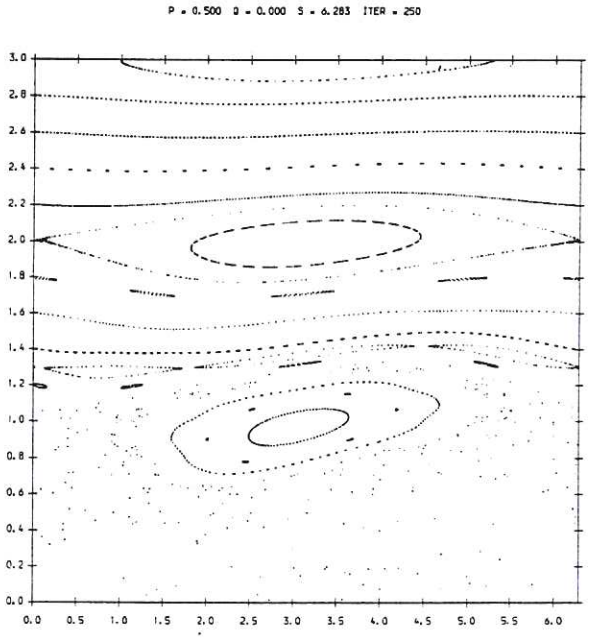

Fig.4

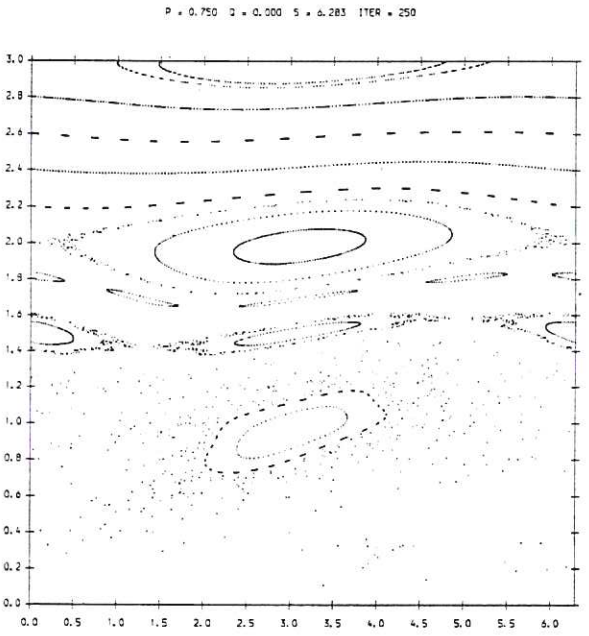

Fig.5

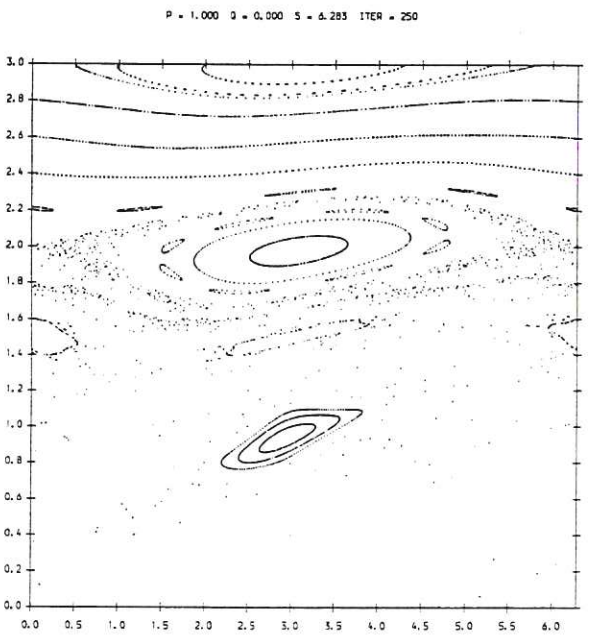

Fig.6

The effect of increasing diffuser strength for a typical Tokamak shear (2π). (Parameter values as indicated).

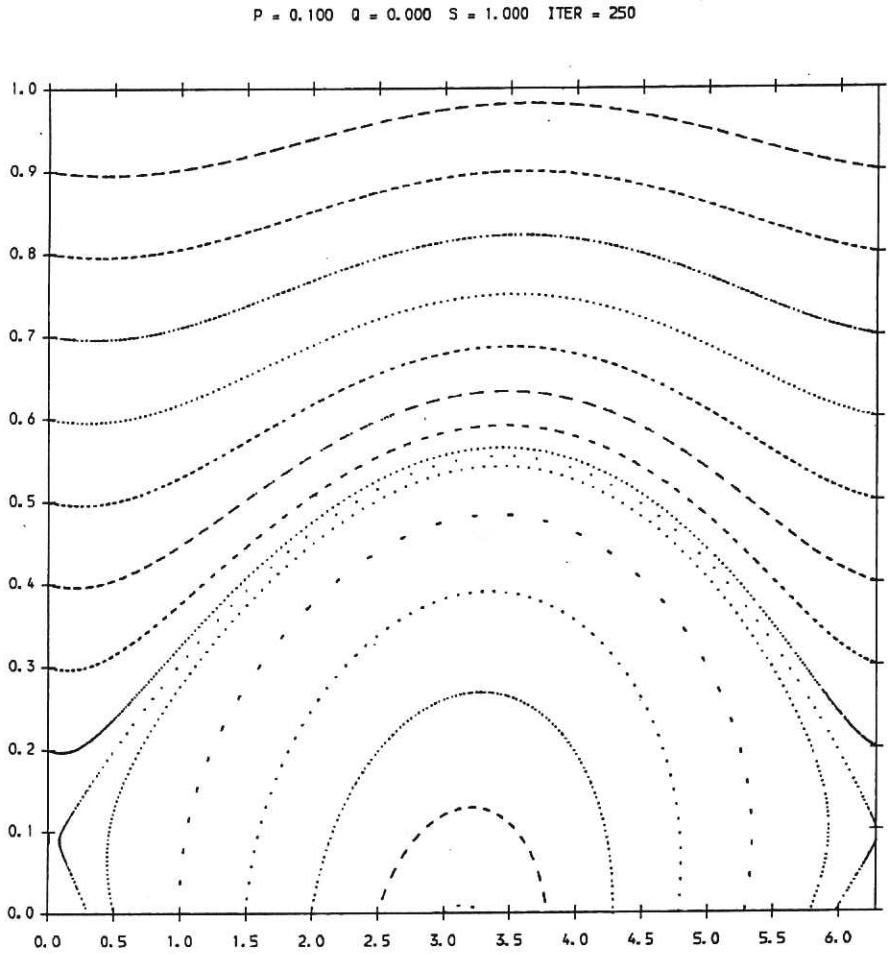

Fig.7 An example of weak shear where there is little evidence of chaotic behaviour.

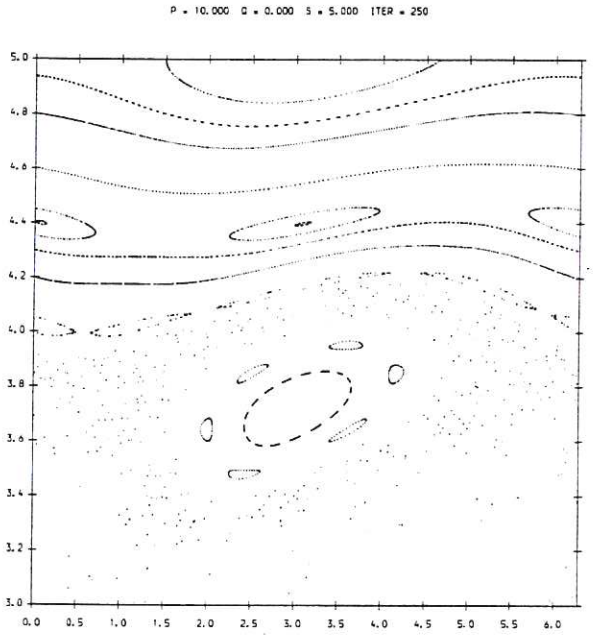

Fig.8

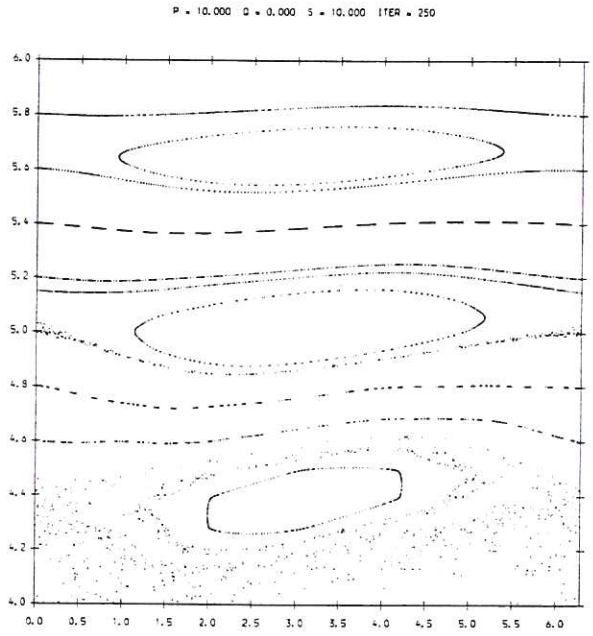

Fig.9

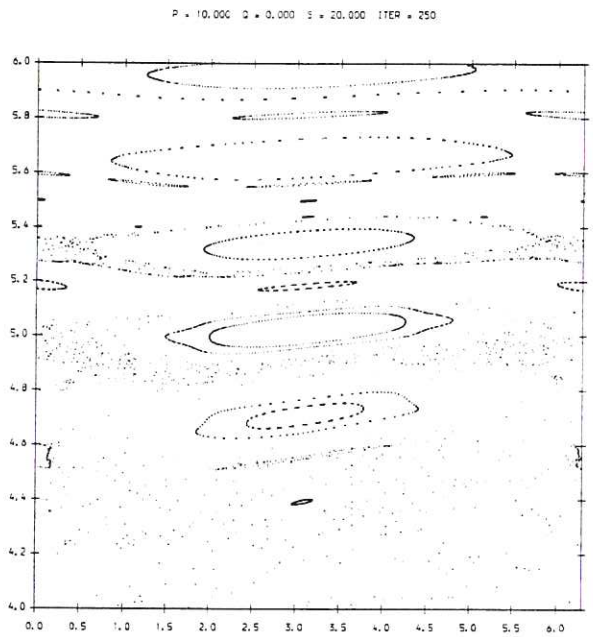

Fig.10

The effect of increasing shear for fixed diffuser strength.
(Parameter values as indicated).

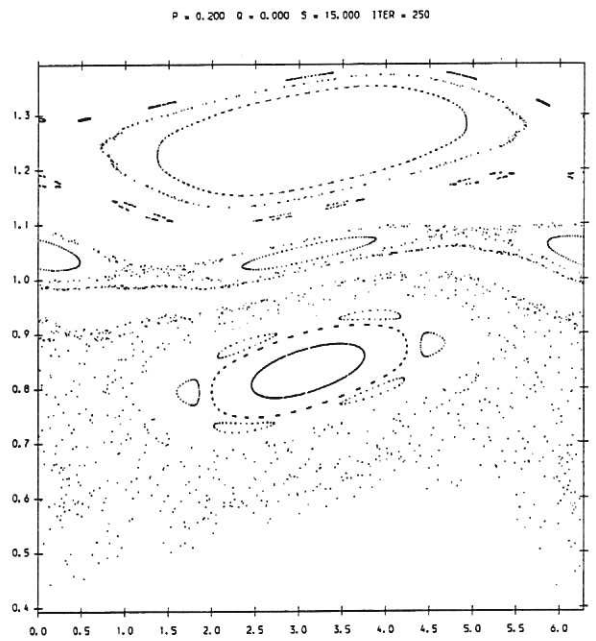

Fig.11

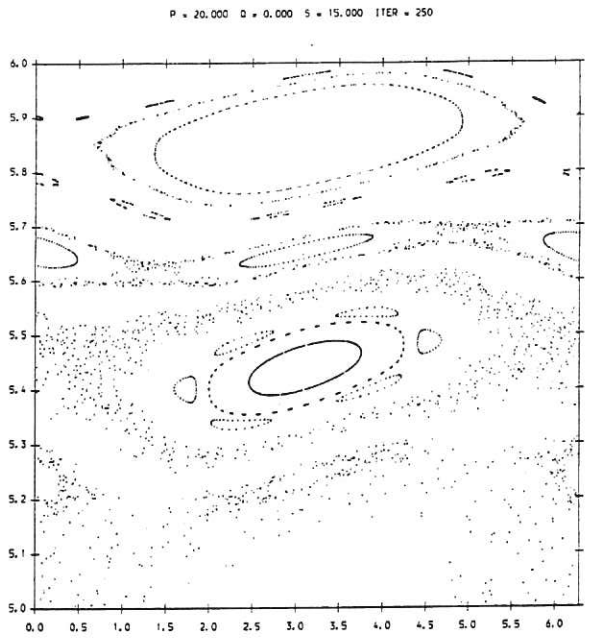

Fig.12

An example of exact pattern replication for widely differing diffuser strengths.

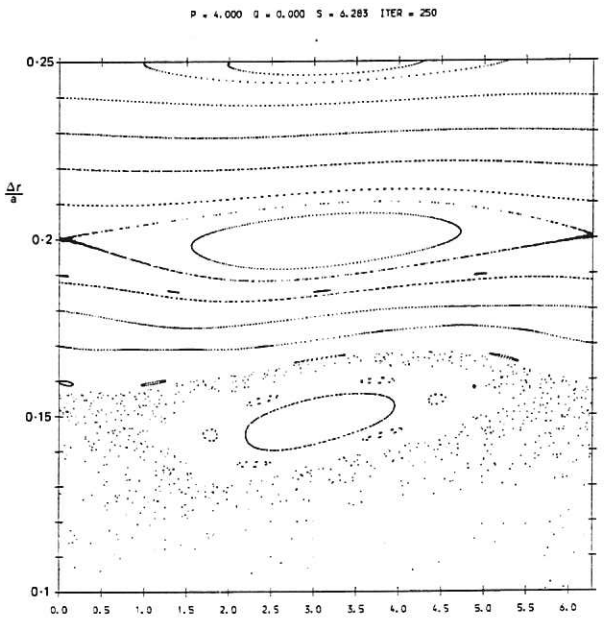

Fig.13 Surfaces generated using JET-like parameters.

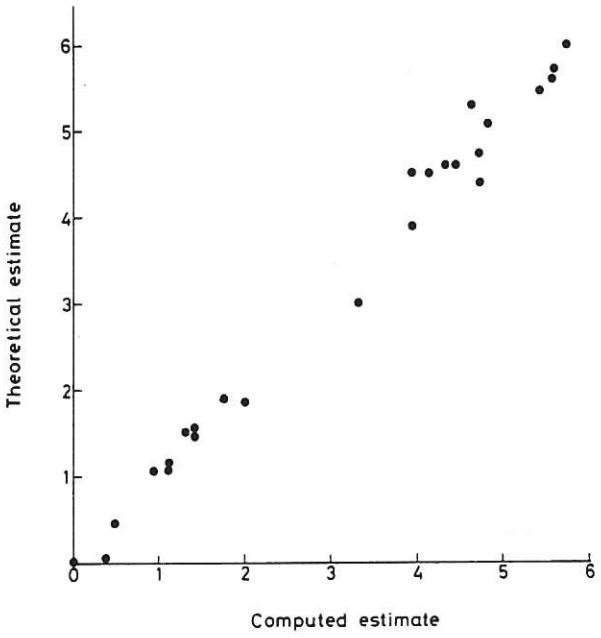

Fig.14 Comparisons of the estimates of the chaotic boundary position from the theoretical and computer model.